

REMOVAL OF THE *GLONASS* C/A SIGNAL FROM OH SPECTRAL LINE OBSERVATIONS USING A PARAMETRIC MODELING TECHNIQUE

STEVEN W. ELLINGSON

ElectroScience Laboratory, Ohio State University, 1320 Kinnear Road, Columbus, OH 43212; ellingson.1@osu.edu

JOHN D. BUNTON

CSIRO Telecommunications and Industrial Physics, P.O. Box 76 Epping, NSW 1710, Australia; jrbunton@tip.csiro.au

AND

JON F. BELL

CSIRO Australia Telescope National Facility, P.O. Box 76 Epping, NSW 1710, Australia; jbell@atnf.csiro.au

Received 2000 October 16; accepted 2001 February 28

ABSTRACT

Astronomers use the 1612 MHz OH spectral line emission as a unique window on galactic dynamics and the properties of evolved stars. In recent years, experiments using this OH line have become more difficult because of interference from the *GLONASS* satellite system. In this paper we demonstrate that the C/A component of the *GLONASS* signal can be removed using a parametric estimation/subtraction technique that exploits known properties of the modulation and requires no additional antennas. Using actual OH line observations, we demonstrate cancellation greater than 20 dB. This technique can be implemented using present-day digital signal processing hardware, and it does not significantly affect the relatively weak astronomy signals or the sensitivity of the measurement.

Subject headings: instrumentation: detectors — methods: analytical — radio lines: general

1. INTRODUCTION

Many papers in the astronomical literature cite problems with interference from the Russian *Global'naya Navigatsionnaya Sputnikovaya Sistema* (*GLONASS*, global navigational satellite system; KNITs 1998¹) when trying to observe 1612 MHz OH spectral line emission. *GLONASS* satellites transmit at frequencies between 1602–1616 MHz and have “shared primary user” status with radio astronomy in the 1610.6–1613.8 MHz band (Combrinck, West, & Gaylard 1994). Each satellite is assigned one of 24 carriers spread over the 14 MHz band at intervals of 562.5 kHz. Both Galt (1991) and Combrinck, West, & Gaylard (1994) present data demonstrating the damaging effect of *GLONASS* signals on astronomy data. Figure 1 of Combrinck et al. (1994) shows time-averaged spectra of these signals. The sidelobes are as high as -25 dB with respect to the main lobe peak, extending out to 20 MHz to either side in some cases (Galt 1991). Some reports have indicated that up to 50% of observations have to be discarded (Galt 1991). The scientific merits of OH spectral line observations are well known (Cohen 1989; Herman & Habing 1985); there is no question that this is extremely valuable spectrum whose continued use is essential to radio astronomy.

One possible solution to the problem is regulation; this is being addressed within international organizations such as the ITU and URSI. However, regulation is unlikely to recover the spectrum into which the *GLONASS* system already transmits. The solution most often employed by radio astronomers in dealing with unwanted signals is to put telescopes in remote locations. However, when dealing with signals that emanate from Earth-orbiting satellites, that method is obviously not effective. Another solution is simply not to observe when interfering signals are present or to throw away affected data (Galt 1991). Some

“*GLONASS* aware” tools have been developed that allow dynamic scheduling of observations in order to minimize interference (Combrinck et al. 1994). However, the strategy of avoidance results in the loss of valuable telescope time; therefore a better solution is desired.

This brings us to signal processing solutions to the problem. There are a number of techniques that have been suggested for removing interference. For example, frequency-domain postcorrelation techniques have been demonstrated on astronomical data (Sault, Ekers, & Kewley 1997;² Kewley, Sault, & Ekers 1999;³ Briggs, Bell, & Kesteven 2000). These techniques are computationally efficient and are “blind” in the sense that no explicit information about the interfering signal—e.g., modulation—is required. However, they operate on the integrated cross spectrum of multiple antenna feeds and thus may be awkward to apply in certain instrumental configurations. Also, at least one of the antennas in this approach must be able to receive the interference with high signal-to-noise ratio, while simultaneously rejecting the astronomical signals of interest. This may be particularly difficult when dealing with satellites. Furthermore, one faces the limitation that correlation is typically done with a very small number of bits per sample; sometimes as few as 1–2 bits. Thus, postcorrelation techniques may be unable to deal with strong satellite interference.

For array telescopes, spatial nulling techniques are a possible solution (Hampson et al. 1998; Leshem & van der Veen 1999;⁴ Ellingson 1999;⁵ Ellingson & Hampson 2002; Leshem, van der Veen, & Boonstra 2000). These techniques may also be applicable to single-dish systems with focal plane arrays. Unfortunately, the various null-forming algo-

¹ See http://www.rssi.ru/SFCSIC/SFCSIC_main.html.

² See <http://www.atnf.csiro.au/SKA/WS>.

³ See <http://www.atnf.csiro.au/SKA/intmit/atnf/conf>.

⁴ See <http://www.nfra.nl>.

⁵ See <http://www.atnf.csiro.au/SKA/intmit/atnf/conf>.

gorithms also involve limitations. These include the requirement for additional antennas, sensitivity to antenna geometry and receiver noise models, and the possibility of beam pattern distortion, which complicates self-calibration.

Time-domain techniques should be better suited in areas where postcorrelation and spatial nulling techniques are limited. However, time domain techniques based on adaptive filtering strategies still face several technical challenges, including problems with noise injection and effectiveness against weak interference (Barnbaum & Bradley 1998). Another class of time-domain techniques attempts to sense the presence of damaging interference and blanks the telescope output accordingly (Leshem et al. 2000). Unfortunately, such techniques are not effective against persistent interference, and they have the effect of reducing the effective integration time when applied to “time division multiplexed” or pulsed signals.

The technique introduced in this paper works in the time domain and operates directly on a single channel of telescope output, with no other inputs required. The technique involves estimating the interference waveform and generating a copy of it, which is simply subtracted from the telescope output. In this way, one can cancel the interference without the possibility of antenna pattern distortion and with no loss of integration time. Apart from the inevitable small errors in estimating the interference waveform, the injected cancelling signal is noiseless. Thus, this technique does not significantly affect the sensitivity of the measurement.

This approach is not without precedent; for example, Miller, Potter, & McCorkle (1997) describe a similar strategy for removing strong terrestrial analog narrowband amplitude- and frequency-modulated signals from ultrawideband radar data. Their strategy was simply to recognize that the interference could be accurately modeled as sinusoids with slowly varying magnitude, phase, and frequency. Estimating these three parameters is a straightforward signal-processing problem; one can then synthesize noise-free replicas that can be subtracted from the contaminated data. However, many satellite signals—including those from *GLONASS*—are digitally modulated and therefore are characterized by different parameters. Furthermore, *GLONASS* is received with relatively low signal-to-noise ratio. Thus, removal of *GLONASS* interference by parametric signal modeling requires a modified approach.

The main limitation of the technique described in this paper is that it is specific to the coarse/acquisition (C/A) component of the *GLONASS* signal, and it will work for no other form of interference without modifications. However, it does appear that this technique can be applied to the wideband component of the *GLONASS* signal, the U.S. Global Positioning System (*GPS*), and possibly a few other signals as well; in each case with only minor modifications. For example, Bunton (2000)⁶ recently demonstrated an extension of the technique described here for mitigating the *GLONASS* wideband component. The relative simplicity and effectiveness of this technique in dealing with the *GLONASS* signal may also make it quite useful as a pre- or postprocessing step for other techniques that experience difficulty mitigating interference due to this signal.

This paper is organized as follows. Section 2 summarizes the properties of the *GLONASS* signal that are relevant to

the operation of the technique. Section 3 describes the theoretical basis for the cancelling technique. The technique itself is presented in § 4. Section 5 describes the procedure used to collect *GLONASS*-corrupted radio astronomy data for evaluation of the technique, and these results are presented in § 6. In § 7, we consider how this approach may be implemented for regular operation on telescope systems.

2. *GLONASS* SIGNAL CHARACTERISTICS

GLONASS, despite its complex wideband spectrum, actually has a very simple structure (KNITs 1998). The signal transmitted from a *GLONASS* satellite consists of two direct sequence spread spectrum (DSSS) components. The first component is a binary phase shift keying (BPSK) modulated C/A signal. This signal is simply a sinusoidal carrier, which experiences a phase shift of 0° or 180° every $(511 \text{ kHz})^{-1} \approx 1.96 \mu\text{s}$. Each phase shift represents a modulation symbol, or *chip*. Each group of 511 chips represents a “pseudorandom noise” (PN) code, which is public knowledge, never changes, and is the same for every *GLONASS* satellite. Data bits are represented by changing the sign of a block of 10 repetitions of the PN code, yielding 100 bits s^{-1} . This signal is typical of DSSS emissions in that it conveys relatively little information per unit bandwidth. This observation is key to the success of the cancelling technique described in this paper.

The second component of the *GLONASS* signal is similar to the C/A component, but is modulated at 10 times the chip rate (5.11 MHz) with a longer PN code. The transmitted power is approximately equal, but because of the higher chip rate the bandwidth is 10 times greater and the power spectral density (e.g., W Hz^{-1}) is 10 dB weaker than that of the C/A component. Therefore, dramatic improvement in the quality of measured spectra is obtained simply by cancelling the C/A component, even if the wideband component is ignored.

A mathematical model for the C/A component of the *GLONASS* signal, as it is transmitted from the satellite, can be written as

$$s_r(t, \omega_c) = c(t - \eta)b(t - \eta)e^{j(\omega_c t + \phi)}, \quad (1)$$

where $c(t)$ represents the PN code, $b(t)$ represents the data bits, ω_c is the center frequency upon transmit, and ϕ represents an arbitrary phase introduced during modulation. $c(t)$ is limited to only two values, +1 and -1, which alternate according to the PN code chips at a rate of $T_c^{-1} = 511 \text{ kHz}$. The PN code [thus $c(t)$] repeats with period $T_p = 1 \text{ ms}$. Since the start times of the PN code are not known a priori, an unknown time offset η is introduced. The data bit stream $b(t)$ is also limited to values of +1 and -1, but changes value no faster than $T_b = 10T_p$ (10 ms). The timing of data bit transitions, like the timing of the PN code, is unknown; however, bit transitions are aligned to fall along code boundaries.

The signal received by the radio telescope can be modeled as

$$s_r(t) = G(t)P(t)s_r(t - \tau, \omega_c + \omega_d), \quad (2)$$

where ω_d is the frequency shift due to the Doppler effect, τ is the propagation time, $P(t)$ is the response of the propagation channel, and $G(t)$ is the radio telescope response. $P(t)$ includes path loss and can be modeled as a single time-varying complex coefficient. $G(t)$ includes the antenna

⁶ See <http://www.jb.man.ac.uk/ska/workshop>.

pattern response, the feed response, and the receiver response. If the radio telescope has bandwidth much greater than *GLONASS*, then $G(t)$ can also be modeled as a single time-varying complex coefficient.

The carrier frequency factor can be removed by multiplying $s_r(t)$ by $e^{-j\omega_c t}$, yielding the low-pass baseband signal

$$s_r^B(t) = G(t)P(t)c(t - \eta - \tau)b(t - \eta - \tau) \times e^{j(-\omega_c \tau + \phi)} e^{j\omega_d(t - \tau)} \quad (3)$$

or simply

$$s_r^B(t) = A(t)c(t - \mu)e^{j\omega_d t}, \quad (4)$$

where $\mu = \eta + \tau$, and

$$A(t) = G(t)P(t)b(t - \mu)e^{j(-\omega_c \tau + \phi)} e^{-j\omega_d \tau}. \quad (5)$$

The above formulation describes the received C/A signal in terms of just three unknown parameters: the Doppler shift ω_d , the “code phase” μ , and a single time-varying complex gain $A(t)$, which accounts for all other effects. This formulation will be exploited later in this paper to provide a simple means for accurately estimating the C/A waveform and synthesizing a suitable replica for cancelling purposes.

Finally, it must be noted that there are important frequency-dependent effects which have not been included in the model as described above. For example, the signal is processed through filters in the satellite which blunt the abrupt phase transitions. The finite bandwidth of the receiver has the same effect. There may also be variations in the frequency response of the transmitter and receiver due to instrumental limitations or multipath effects. From the perspective of the radio telescope output, the aggregate effect of all of these phenomena can be described in terms of a single complex-valued response function, $H(\omega)$. As we shall see later, $H(\omega)$ changes very slowly, and it is not necessary to know $H(\omega)$ in order to accurately estimate the signal parameters. It will, however, be important to account for $H(\omega)$ when constructing a cancelling signal.

3. ESTIMATION AND SYNTHESIS OF THE C/A SIGNAL

As described earlier, two important tasks in our technique are to estimate the parameters of the C/A signal and to determine the unmodeled portion of the frequency response. The following sections describe theory and procedures for estimation of the time-varying signal parameters A , μ , ω_d and the system response $H(\omega)$.

3.1. Parameter Estimation

The formulation developed earlier leads to a simple method for estimation the parameters ω_d , μ , and A . Let $x(t)$ be the signal received by the telescope. A “cost function” $J(\mu, \omega_d)$ is formed from the correlation of $x(t)$ with $s_r^B(t)$ as follows:

$$J(\mu, \omega_d) = \frac{1}{T_J} \int_t^{t+T_J} x^*(t) s_r^B(t - \mu, \omega_d) dt, \quad (6)$$

where T_J is the correlator length, selected using the rule of thumb that $T_p \leq T_J \ll T_b$. Choosing T_J as small as possible minimizes the probability that $x(t)$ includes a sudden sign change due to a change in the data bit, which reduces the peak correlation magnitude. This is not a serious problem unless the data bit changes sign close to the center of the

correlation period, in which case the peak correlation approaches zero. This problem is easily avoided by either (1) performing the search at least twice, using data offset in time by T_p or (2) using new data at each step in the search, so that the problem appears as an isolated glitch in the surface $J(\mu, \omega_d)$ and can be detected. Since T_b is only 10 times T_p for the *GLONASS* C/A code, $T_J = T_p$ is recommended.

Since this correlation will typically be done digitally, it is perhaps more appropriate to redefine $J(\mu, \omega_d)$ as

$$J(\mu, \omega_d) = \frac{T_S}{T_J} \sum_{k=1}^{T_J/T_S} x^*(kT_S) c(kT_S - \mu) e^{j\omega_d kT_S}, \quad (7)$$

where k is a sample index and T_S is the sample period. Note that we have now left out $A(t)$, assuming it is approximately constant over the correlation time.

To estimate μ and ω_d given $x(t)$, one seeks the values of μ and ω_d that maximize $J(\mu, \omega_d)$; i.e.,

$$\{\hat{\mu}, \hat{\omega}_d\} = \arg \max_{\mu, \omega_d} J(\mu, \omega_d). \quad (8)$$

If μ and ω_d are completely unknown, this amounts to a two-dimensional brute-force search, and it is known as “acquisition.” At first glance, this may seem to be a dauntingly complex task; however, it is essentially the same procedure used by *GLONASS* and *GPS* receivers when they are first turned on. Once acquisition is achieved, updating μ and ω_d is simple because they vary slowly. These parameters can be tracked simply by sensing the drift in the correlation peak and adjusting the parameters accordingly. A detailed procedure is suggested later in this paper.

Given $x(t)$ and the estimates $\hat{\mu}$ and $\hat{\omega}_d$, one finds

$$\hat{A} = J(\hat{\mu}, \hat{\omega}_d). \quad (9)$$

Note that this is a single correlation (not a search) and thus can be computed quite efficiently. This is fortunate since A is expected to change rapidly relative to μ and ω_d . In the examples presented later in this paper, the complex gain update rate is 128 μ s.

3.2. Finding $H(\omega)$

In § 2, it was pointed out that bandpass correction was necessary to account for a nonflat $H(\omega)$. In this section, we describe a method for computing this correction.

Our method begins with an estimate of the baseband C/A signal $\hat{s}_r^B(t)$, generated using the estimated signal parameters substituted into equation (4). Note that

$$s_r^B(t) = h(t) * \hat{s}_r^B(t), \quad (10)$$

where the asterisk denotes convolution and $h(t)$ is the inverse Fourier transform of $H(\omega)$ and has the physical interpretation of being the impulse response. $\hat{s}_r^B(t)$ is effectively noiseless, whereas the received signal $x(t)$ can be modeled as $s_r^B(t)$ plus a noise component $n(t)$. In the frequency domain, the correlation of the received signal with the synthesized (estimated) signal is given by

$$R_{x_s}(\omega) = \langle [S_r^B(\omega) + N(\omega)] [\hat{S}_r^B(\omega)]^* \rangle, \quad (11)$$

where the angle brackets denote the statistical expectation, and uppercase symbols are used to denote the Fourier transform of the quantities associated with the lowercase counterparts. If the noise is uncorrelated with any other component of the signal and has zero mean, this expression

reduces to

$$R_{xs}(\omega) = H(\omega)R_{ss}(\omega), \quad (12)$$

where

$$R_{ss}(\omega) = \langle \hat{S}_r^B(\omega)[\hat{S}_r^B(\omega)]^* \rangle. \quad (13)$$

Note that $R_{ss}(\omega)$ can be computed once the estimate $\hat{S}_r^B(t)$ is available, and that $R_{xs}(\omega)$ can be computed using $\hat{S}_r^B(t)$ and $x(t)$. Then, $H(\omega)$ is simply $R_{xs}(\omega)/R_{ss}(\omega)$.

Given $H(\omega)$, the inverse Fourier transform yields $h(t)$, which can be sampled to obtain the coefficients for a transversal digital filter. Passing $\hat{S}_r^B(t)$ through this filter yields a signal that closely resembles the C/A signal present in the telescope output and therefore can be subtracted to achieve cancellation.

4. C/A REMOVAL TECHNIQUE

The actual procedure consists of two phases. The first phase is acquisition. This involves a search for initial values of ω_d and μ , using the method implied by equation (8). This is exactly the same task performed by commercial satellite navigation receivers, and requires on the order of 10 s. This is followed by a calculation of the end-to-end frequency response $H(\omega)$, using the method implied by equation (12). Once acquisition is complete, the procedure enters the “tracking” phase, shown in Figure 1. Tracking is the normal mode of operation; acquisition is required only once (as a satellite appears), and does not need to be repeated.

In tracking, estimates of μ and ω_d must be updated on a timescale of 1–10 ms. Let us first consider the $\hat{\mu}$ update. There are a number of techniques used in DSSS systems for

code phase tracking. For this application, “delay-lock tracking” (Dixon 1984) gives good performance. This is implemented by calculating the correlation metrics

$$K_{\text{early}} = |J(\hat{\mu} - T_c/2, \hat{\omega}_d)| \quad (14)$$

and

$$K_{\text{late}} = |J(\hat{\mu} + T_c/2, \hat{\omega}_d)|, \quad (15)$$

in addition to $K_{\text{prompt}} = |\hat{A}|$. Choosing a value of exactly $T_c/2$ is not critical; normally one simply chooses the closest integer number of sample periods. If $\hat{\mu}$ is perfect, then K_{prompt} will be greater than K_{early} and K_{late} , and $K_{\text{early}} \approx K_{\text{late}}$. If $|K_{\text{late}} - K_{\text{early}}|$ exceeds one eighth of their mean value, then $\hat{\mu}$ is adjusted by one period of the sample clock. Correlation metrics are calculated every sample and then averaged with a first-order low-pass filter to reduce noise and prevent unnecessary code phase changes (“jittering”).

The Doppler shift ω_d is tracked by manipulating the phase of the LO shown in Figure 1. This phase changes very slowly; experiments have shown that the update period can be as long as 3 ms. The C/A signal has only two modulation states; the transmitted carrier phase is either 0° or 180° . The current state is conveyed by the phase of \hat{A} . It is a simple matter to compute the drift in the phase of \hat{A} from update to update; then the phase shift required by the LO for Doppler tracking is simply the negative of this drift. Note that *GLONASS* data bit boundaries have to be avoided to prevent ambiguity; however, these boundaries are well-separated (10 ms) and are easy to identify and work around in practice.

5. TEST DATA

To test our technique, we used observations of the OH maser OH 354.88–0.54 (Caswell et al. 1981; Jones et al.

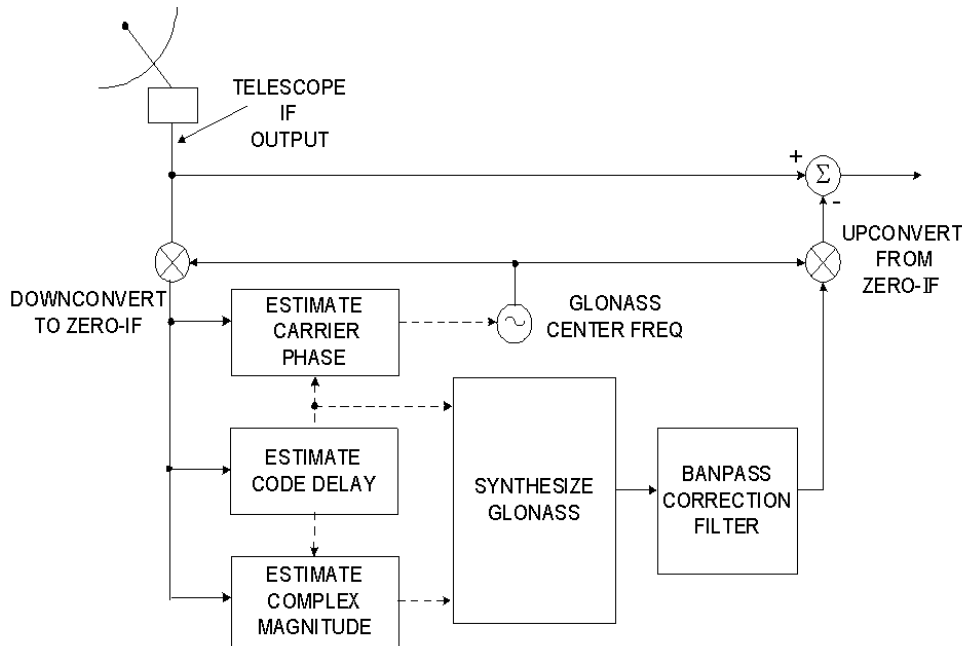


FIG. 1.—Technique for removal of the *GLONASS* C/A signal from radio telescope output (tracking mode). First, an updated estimate of the code delay μ is obtained and used to generate a time-aligned replica of the PN code. μ is used along with the down-converted telescope output to estimate the complex magnitude A . μ and A are then used to synthesize the *GLONASS* C/A waveform $\hat{S}_r^B(t)$. This output is then conditioned to account for $H(\omega)$ (bandpass correction), using a transversal filter. This results in a replica of the C/A signal, but centered at zero-IF. At the same time, an updated estimate of ω_d (equivalently, the carrier phase) is calculated and is used to adjust the frequency of a complex-valued digital local oscillator (LO). This LO is used to center the C/A signal at zero-IF for estimation/synthesis, and to return the synthesized cancelling signal to the original center frequency in the IF. The up-converted synthesized C/A signal is subtracted from the telescope output to effect the removal of the interference.

1982), also known as IRAS 1731 – 33, at ~ 1612.15 MHz by the six 22 m dishes of the Australia Telescope Compact Array (ATCA) at Narrabri, New South Wales. A single linear polarization was captured from each dish, sampled using four levels at 16 million samples per second (MSPS) and recorded on an S2 recorder (Cannon et al. 1997). The resulting bandpass was 8 MHz wide centered at 1610 MHz. The data were then extracted using the S2TCI system (Wietfeldt et al. 1998) and demultiplexed. This data set and others are freely available (Bell et al. 2000). A portion of this observation was corrupted by the signal from *GLONASS*-69 at ~ 1609 MHz, entering through a far sidelobe.

6. RESULTS

First, the data from one of the ATCA dishes were used to test our *GLONASS* C/A cancelling technique. The results are encouraging, with *GLONASS* C/A signals being effectively removed in a way that does not appear to affect the astronomy signals. Figure 2 shows a spectrum of the raw data with the OH maser visible at 1612.15 MHz and the C/A component of the interference from *GLONASS*-69 visible at 1609 MHz. For diagnostic purposes, we added a test tone (via software), which is visible at 1611.3 MHz. This plot represents 4.8 s of integration, in one case with the canceller on and in the other with the canceller off. When the canceler is on, the C/A signal and its sidelobes within the observing band are removed.

The amount of the C/A signal remaining after cancellation was estimated from the variation in the “after” spectrum, after baseline removal. The result, shown in Figure 3, indicates a variation of less than 5 units peak. By the same scale, the peak of the “before” C/A spectrum is about 550 units after baseline removal. From this, we estimate of the ratio of C/A signal power “before” versus “after” to be at least 20 dB, but less than 25 dB.

Another test of the performance of the cancelling technique is to cross-correlate the canceller output with signals from another antenna from the ATCA which has not been processed using the canceller. If any *GLONASS* signal remains, this test should reveal a strong signature. Figure 4 shows the results of this test. The test tone was not used in

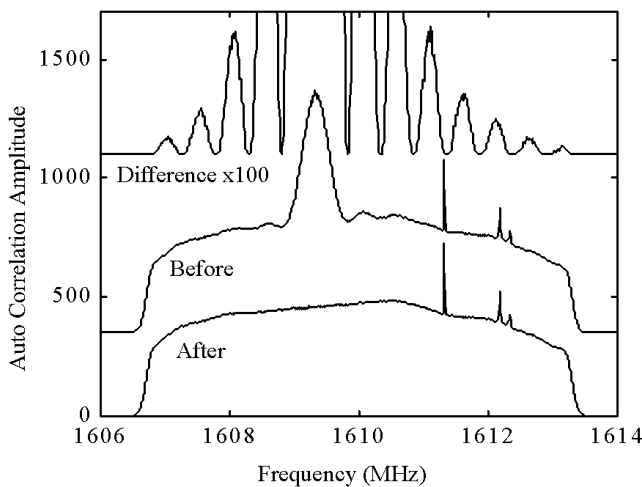


FIG. 2.—Middle curve: Autocorrelation of raw data, including (left to right) *GLONASS*, test tone, and OH maser. Bottom curve: Same signal after processing (C/A signal removed). Top curve: The cancelled signal (i.e., “before”-“after”) multiplied by 100, showing the spectrum of the signal that was cancelled (curves offset for clarity).

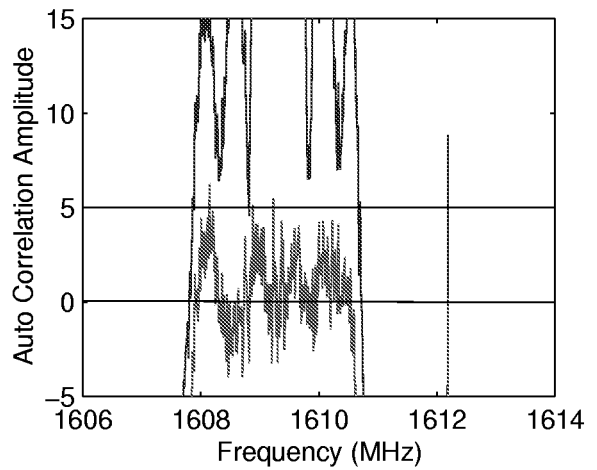


FIG. 3.—“Before” (top curve) and “after” (bottom curve) spectrum, after baseline removal in both cases. The “before” spectrum has been shifted up 7.5 units for clarity.

this experiment. It is clear that the *GLONASS* C/A signal has been mostly removed.

What remains is dominated by the wideband component of the *GLONASS* signal, which we have not tried to suppress. Nevertheless, C/A-only cancellation is worthwhile as the baseline of the resulting spectra varies less quickly, and therefore allows greatly improved baseline estimates and easier identification of weak spectral features throughout the band.

In the results above, the canceller has no noticeable effect on the OH maser or the test tone. In other words, the cancelling technique does not appear to be “toxic” to the astronomy signal, or to the test tone. However, these signals were located in the far sidelobes of the C/A signal. In order to examine the toxicity of this algorithm in the main lobe of the C/A signal, we added some additional test signals. As shown in Figure 5, we added a second test tone and also a narrowband noise signal, synthesized in software, intended to model spectral features commonly of interest in radio

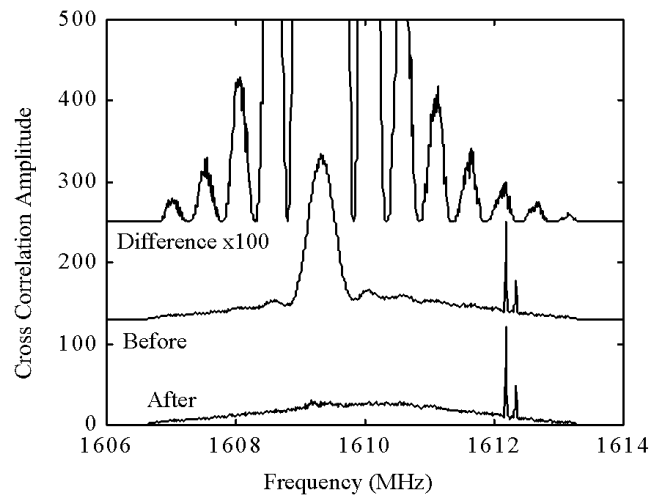


FIG. 4.—Middle curve: Cross-correlation of raw data from two antennas. Bottom curve: Cross-correlation of raw data from one antenna with data from another antenna which were processed by the canceller. Top curve: Cancelled (difference) signal multiplied by 100, showing the spectrum of the signal that was cancelled (curves offset for clarity).

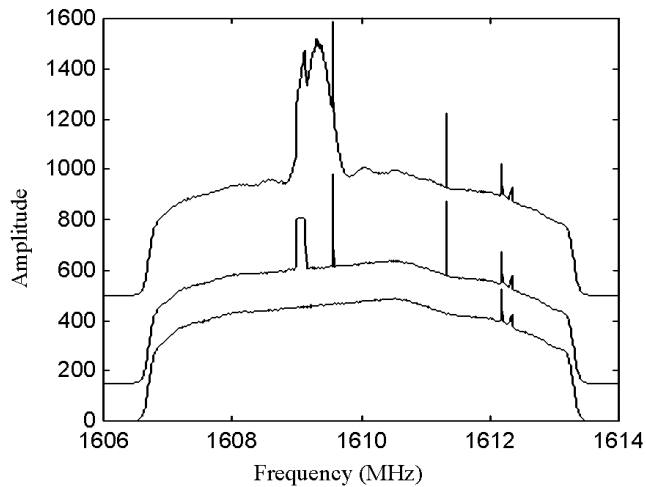


FIG. 5.—*Top curve*: Narrowband noise and second tone added before cancellation. *Middle*: After cancellation of the C/A signal. *Bottom*: Cancellation of C/A signal followed by subtraction of all additional test signals (*curves offset for clarity*).

astronomical observations. Figure 5 shows the result of subtracting the additional test signals after the cancellation. Note that there is no evidence that these signals have been affected by the cancellation—otherwise some of the distorted signal would remain after subtraction. Therefore, the canceller appears to be nontoxic even to signals within the main lobe of the C/A signal.

We also considered the performance of the canceller with versus without test signals near the *GLONASS* center frequency, by taking the difference of the bottom curves of Figures 2 and 5. The result is shown in Figure 6. We note that the residual structure evident in this spectrum is about -30 dB or 0.1% (1 part in 1000) of the original *GLONASS* signal. The incomplete cancelling is due to the presence of the test signals, which have a combined power of roughly 20% of the power of the *GLONASS* main lobe. These signals introduce “structured noise” into the correlation process used to estimate the *GLONASS* signal. As a result,

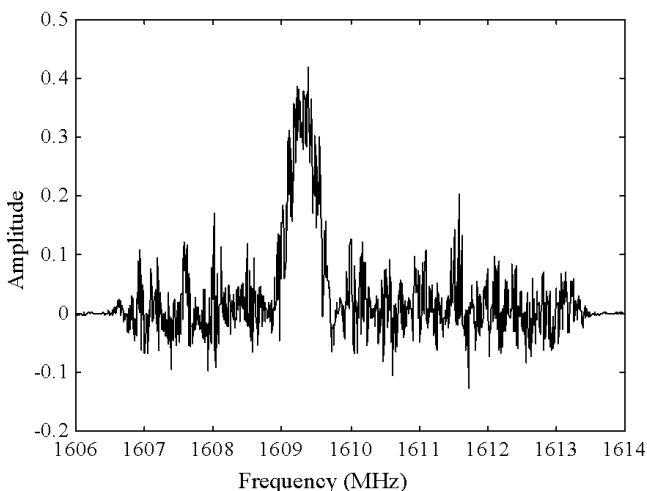


FIG. 6.—Difference of the output autocorrelation spectrum when the processing was run with and without the presence of the test tone and band limited noise near the *GLONASS* center frequency. Test signals were subtracted before taking the difference.

the accuracy of the cancellation has been reduced. The RMS noise in the rest of the spectrum is at a level of -40 dB relative to the *GLONASS* signal. We conclude that processing with or without the presence of other signals in the main lobe of the *GLONASS* signal makes very little difference in the effectiveness of the canceller. Since the canceller is not significantly influenced by the presence of astronomy signals, it is unlikely to create spurious processing “artifacts” or otherwise misleading results within the limits identified above.

The analysis described above has been repeated independently for each of six antennas of the ATCA. The results presented above are typical.

7. IMPLEMENTATION AND OTHER APPLICATIONS

To date, the technique has been implemented only in the form of non-real-time postprocessing software, written in MATLAB. The source code is freely available from the authors. By these means, the processing runs at about 1000 times real time on a 400 MHz Pentium desktop computer. Any practical system would, of course, require real-time implementation. Fortunately, techniques and hardware for the processing of *GLONASS* and *GPS* signals are well developed (Dixon 1984; Kaplan 1996). In fact, the acquisition and tracking procedures described in §§ 3 and 4 are basically the same as those used in low-cost commercial receivers for *GLONASS*, *GPS*, and cellular CDMA telephones, using similar data rates. Thus, practical real-time implementation seems to be within reach.

The hardware needed to implement the canceller is commonly available. Synthesis of the cancelling signal is straightforward using present-day field programmable gate array (FPGA) technology, whereas parameter estimation and tracking functions can be implemented within a programmable digital signal processing (DSP) chip, such as the those available from companies, including Texas Instruments and Analog Devices. The main difficulty in the parameter estimation are the correlations, which are simple but tedious. However, once acquisition has been achieved, the computational burden associated with these correlations is dramatically reduced; an order-of-magnitude estimate is 200 million floating-point operations per second at 8 MSPS, which is well within the capabilities of commercially available DSP microprocessors. Furthermore, it is possible to use FPGAs for these correlations, which relieves the DSP microprocessors of this burden.

We can imagine two means by which the canceller could be used with radio telescopes. The most elegant approach is to build new receivers that incorporate this technique. However, the technique seems also to be well-suited to implementation in the form of an appliqué, or “add-on,” to existing systems.

Finally, we note that there appear to be many applications for the parametric signal modeling approach beyond cancelling the *GLONASS* C/A signal. As mentioned previously, the wideband component of the *GLONASS* signal is similar in format, with the main difference being a longer PN code with faster chip rate. The modulation used by the *GPS* is very similar to the modulation used in the *GLONASS* (Kaplan 1996). The main differences in the C/A mode of the *GPS* signal are longer PN code (1023 chips) and higher chip rate (1.023 MHz); also, all *GPS* satellites transmit on the same center frequencies, but with different (but known) PN codes. Thus, techniques that are effective

against the *GLONASS* C/A signal are likely to be directly applicable to the *GPS* C/A signal as well. In addition to *GLONASS* and *GPS*, many other satellite and terrestrial systems for navigation and communications use well-specified DSSS modulation formats. These forms of interference are likely to yield to the same cancelling strategy.

However the details, and possibly the implementation, will be different in each case.

The authors gratefully acknowledge productive discussions with R. Fisher, R. Ekers, P. Hall, R. Sault, F. Briggs, M. Kesteven, and W. Wilson.

REFERENCES

- Barnbaum, C., & Bradley, R. F. 1998, *AJ*, 116, 2598
 Bell, J. F., Ekers, R. D., & Bunton, J. D. 2000, *Proc. Astron. Soc. Australia*, 17, 255
 Briggs, F. H., Bell, J. F., & Kesteven, M. J. 2000, *AJ*, 120, 3351
 Bunton, J. D. 2000, in *Technological Pathways to the Square Kilometer Array* (Manchester, UK: Jodrell Bank Observatory)
 Cannon, W. H., et al. 1997, *Vistas Astron.*, 41, 297
 Caswell, J. L., et al. 1981, *Australian J. Phys.*, 34, 333
 Cohen, R. J. 1989, *Space Policy*, 5, 91
 Combrinck, W. L., West, M. E., & Gaylard, M. J., 1994, *PASP*, 106, 807
 Dixon, R. C. 1984, *Spread Spectrum Systems* (New York: Wiley)
 Ellingson, S. W. 1999, in the *Elizabeth and Frederick White Conference on Radio Frequency Interference Mitigation Strategies*, ed. J. F. Bell & L. Kewley (Sydney: CSIRO)
 Ellingson, S. W., & Hampson, G. A. 2002, *IEEE Trans. on Antennas and Propagation*, in press
 Galt, J. 1991, in *ASP Conf. Ser. 17, Light Pollution, Radio Interference, and Space Debris*, ed. D. L. Crawford (San Francisco: ASP), 13
 Hampson, G. A., Goris, M., Joseph, A., & Smits, F. 1998, in *Digital Signal Processing Workshop* (Bryce Canyon, AZ: IEEE)
 Herman, J., & Habing, H. J. 1985, *A&SS*, 59, 523
 Jones, T. J., et al. 1982, *ApJ*, 523, 208
 Kaplan, E., ed. 1996, *Understanding GPS: Principles and Applications* (New York: Artech)
 Kewley, L., Sault, R. J., & Ekers, R. D. 1999, in the *Elizabeth and Frederick White Conference on Radio Frequency Interference Mitigation Strategies*, ed. J. F. Bell & L. Kewley (Sydney: CSIRO)
 KNITs. 1998, *GLONASS Interface Control Document* (Moscow: Russian Fed. Ministry Defense)
 Leshem, A. & van der Veen, A.-J. 1999, in *Technologies for Large Antenna Arrays*, ed. M. P. van Haarlem & B. Smolders (Dwingeloo: Astron)
 Leshem, A., van der Veen, A.-J., & Boonstra, A.-J. 2000, *ApJS*, 131, 355
 Miller, T., Potter, L., & McCorkle, J. 1997, *IEEE Trans. Aerospace & Electronic Systems*, 33, 1142
 Sault, R. J., Ekers, R. D., & Kewley, L. 1997, in *1 kT Technical Workshop*, ed. W. Brouw (Sydney: CSIRO)
 Wietfeldt, R., van Straten, W., del Rizzo, D., Bartel, N., Cannon, W., & Novikov, A. 1998, *A&AS*, 131, 549